

Zhijiang WU, Chenfei SONG, Jian GUO, Bingjun YU, Linmao QIAN

A multi-probe micro-fabrication apparatus based on the friction-induced fabrication method

© Higher Education Press and Springer-Verlag Berlin Heidelberg 2013

Abstract A novel multi-probe micro-fabrication apparatus was developed based on the friction-induced fabrication method. The main parts of the apparatus include actuating device, loading system, and control system. With a motorized *XY* linear stage, the maximum fabrication area of 50 mm × 50 mm can be achieved, and the maximum sliding speed of probes can be as high as 10 mm/s. Through locating steel micro balls into indents array, the preparation of multi-probe array can be realized by a simple and low-cost way. The cantilever was designed as a structure of deformable parallelogram with two beams, by which the fabrication force can be precisely controlled. Combining the friction-induced scanning with selective etching in KOH solution, various micro-patterns were fabricated on Si(100) surface without any masks or exposure. As a low-cost and high efficiency fabrication device, the multi-probe micro-fabrication apparatus may encourage the development of friction-induced fabrication method and shed new light on the texture engineering.

Keywords friction-induced fabrication, silicon, surface texture, friction, multi-probe

1 Introduction

Micro/nano-textured silicon has been widely used in micro/nano electromechanical systems (MEMS/NEMS) [1,2], nanoimprint lithography (NIL) templates [3,4], silicon solar cells [5], optoelectronic devices [6], and so on. As a typical micro/nano fabrication method on silicon, lithography was restricted by its involute processes and

poor resolution [7]. In addition, the cost of the up-to-date lithography equipments was far from being acceptable [8]. Therefore, it remains very important to develop efficient and low-cost fabrication methods for surface texture engineering.

Recently, a friction-induced fabrication method was developed by Yu et al. [9], by which three dimensional nanostructures can be directly produced on silicon surface by scanning a diamond tip on target area. Based on the selective etching of such friction-induced structures, various nanostructures can be generated on silicon and quartz surfaces [9,10]. Since this method is independent on the etching masks or exposure, it can be a potential efficient micro/nano fabrication technology. However, as the current friction-induced fabrication was mainly accomplished on the atomic force microscope (AFM) with single-point contact mode [9–11], both the scan speed and fabrication area are limited by the scanner [12]. Therefore, it is essential for us to develop a multi-probe device to improve the fabrication efficiency of friction-induced method.

In this paper, a multi-probe micro-fabrication apparatus was developed based on the friction-induced fabrication method. The working principle and key designs of the apparatus were introduced detailedly. The capability of the multi-probe micro-fabrication apparatus was demonstrated by the fabrication of textures on silicon. As a low-cost and high efficiency fabrication device, the multi-probe micro-fabrication apparatus may encourage the development of friction-induced fabrication method and shed new light on the texture engineering.

2 Working principle of the apparatus

The working principle of the apparatus is shown in Fig. 1. Figure 2 shows the image of the mechanical part of apparatus. As shown in Figs. 1 and 2, the main parts of the apparatus include actuating device, loading system, and control system. The multi-probe array was fixed on the

Received May 28, 2013; accepted July 2, 2013

Zhijiang WU, Chenfei SONG, Jian GUO, Bingjun YU,

Linmao QIAN (✉)

Tribology Research Institute, Key Laboratory of Advanced Technologies of Materials, Ministry of Education, Southwest Jiaotong University, Chengdu 610031, China

E-mail: linmao@swjtu.edu.cn

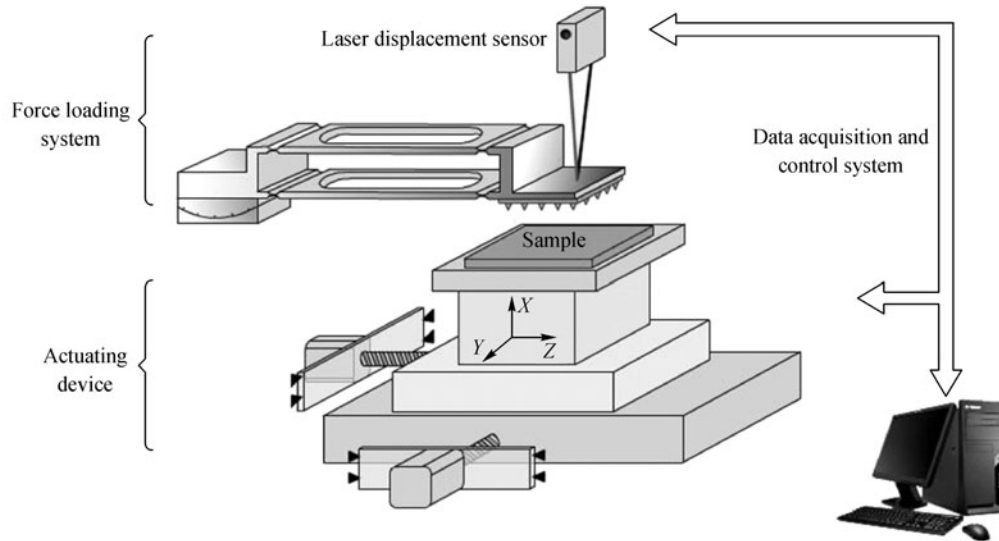


Fig. 1 Sketch of the multi-probe micro-fabrication apparatus

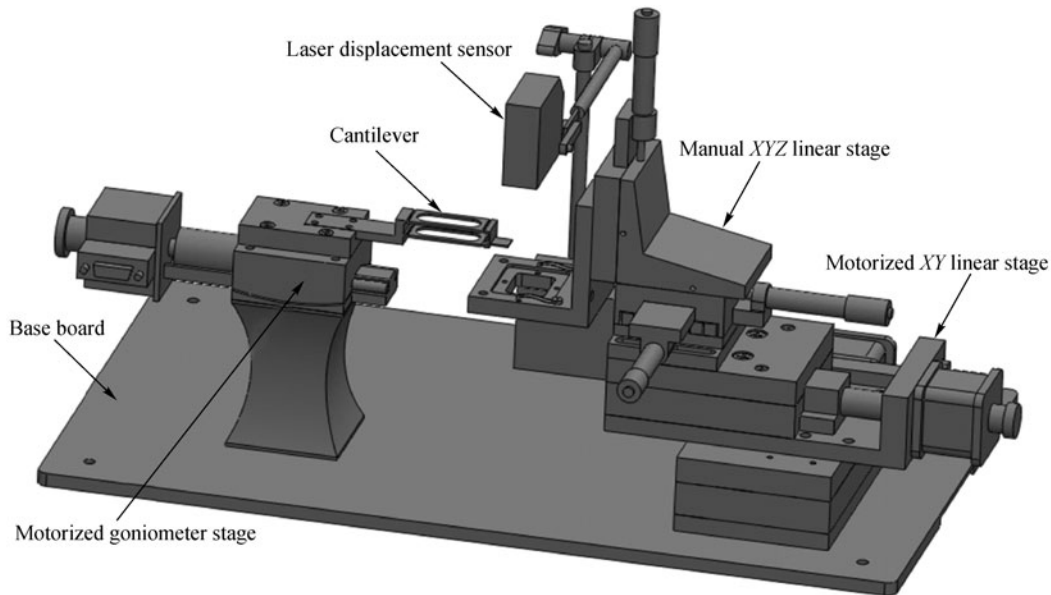


Fig. 2 Image of the mechanical part of apparatus

lower surface of cantilever. The position of sample can be adjusted by two motors and a manual XYZ linear stage. When a normal force is applied on the sample surface by the multi-probe array, an upward movement of cantilever will take place. By using a laser displacement sensor, the deflection of cantilever can be detected and the normal force can then be obtained. The signals from the laser displacement sensor are transferred to the computer through the data acquisition and control system.

Before the fabrication, the sample is first moved up by adjusting the XYZ linear stage until the normal load reaches the target value. After that, the friction-induced fabrication

process will be controlled by computer, which will send out the scanning signals to the motors through the data acquisition and control system to move the sample along a designed trace. Finally, the demanded patterns can be fabricated on the target area.

3 Key designs of the apparatus

As a multi-probe micro-fabrication apparatus, one of the most important designs is to realize the multipoint contact. In addition, since the contact pressure and controllable

scanning are two necessary conditions for the friction-induced fabrication, precisely loading and scanning actuating are also two key designs for the apparatus.

3.1 Multipoint contact

The multipoint contact was realized through the multi-probe array. The number of probes directly affected the fabrication efficiency. The manufacturing process of multi-probe array was schematically shown in Fig. 3.

1) Produce the indents array on a wax substrate by a Vickers hardness tester (Akashi, model MVK-H21, Japan) according to the requirement. The well-ordered indents will be served as the sites of the micro probes (Fig. 3(a)).

2) Place the micro probes (steel micro balls) on the indents (Fig. 3(b)).

3) Press the micro balls with a quartz sheet to make the top of the balls on a horizontal plane. The indentation depth of the balls was usually set as the radii of the steel balls (Fig. 3(c)).

4) Box the wax substrate by a cuboid-shaped wax mold (Fig. 3(d)).

5) Pour the denture base polymers into the mold to cover the balls array. The solidification period was 120 min at least (Fig. 3(e)).

6) Remove the wax mold and wax substrate by heating at 373 K. Polish the bare side of the curdled polymer (Fig. 3(f)).

Finally, the multi-probe array was mounted on the lower surface of cantilever. Since the cantilever was further fixed on a motorized goniometer stage, compensation adjustment of the multi-probe array could be realized by rotating the motorized goniometer stage.

3.2 Precisely loading

Precisely loading is important for the friction-induced micro/nano fabrication process. Due to its anti-oxidation and high strength property, 316L stainless steel was utilized as cantilever material. The structure of cantilever was designed as deformable parallelogram with two beams [13]. Compared to a single beam, the deformable parallelogram makes the cantilever deflect with smaller angles under the same normal load. Moreover, the deflection of the cantilever is more linear with the vertical strain [14], so that the linearity of the force measurement system is guaranteed.

As shown in Fig. 4(a), the cantilever was made from one piece of bulk stainless steel. The bulk stainless steel was first covered out to make an original cantilever containing two beams. Each beam had a thickness of 1.5 mm, width of 18 mm and length of 56 mm. A thin plat of 10 mm \times 10 mm came out at the apex of the bottom cantilever so that the multi-probe array can be fixed onto it. After that, semicircular grooves were cut at both sides of the each beam apex, resulting in the thinnest part of the single beam in thickness of 0.15 mm, as shown in Fig. 4(b). After these processes, the spring constant of the cantilever was calculated as 6309 N/m by the finite-element analysis. To achieve the aforementioned objectives, central parts of the beams and the thinnest parts were further hollowed to reduce the spring constant to 1560 N/m, as shown in Fig. 4(c).

Before the friction-induced fabrication, the cantilever (see Fig. 5) needs to be calibrated on the multi-probe micro-fabrication apparatus. The standard weights with different mass were hanged at the apex of the cantilever

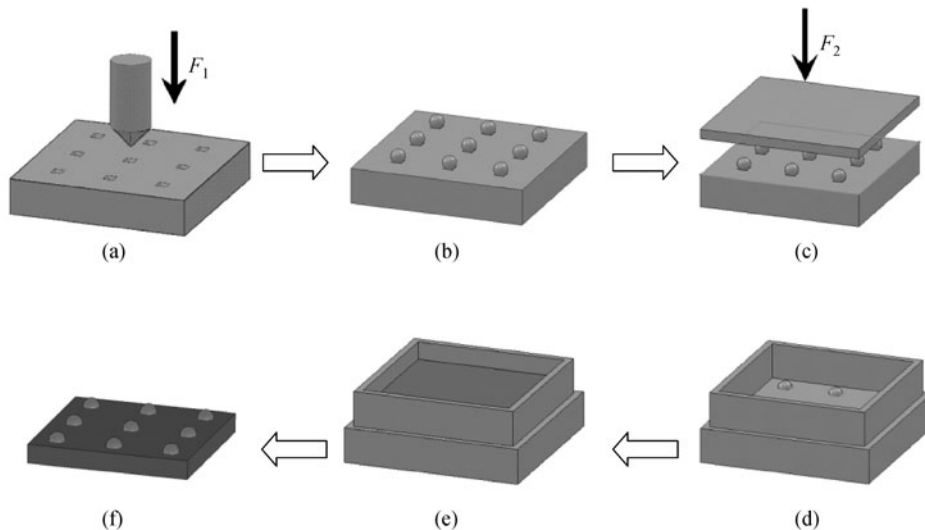


Fig. 3 Manufacturing of multi-probe array. (a) Producing the indents array; (b) placing micro probes; (c) flattening the micro probes; (d) envelopment by the wax mold; (e) founding; (f) substrate polishing

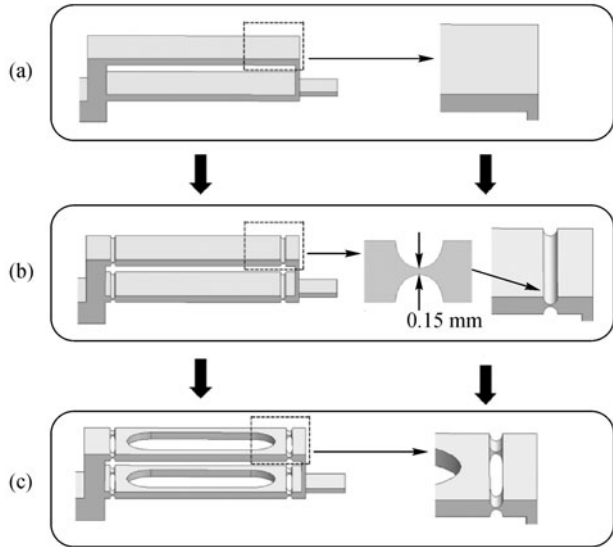


Fig. 4 Fabrication of the cantilever. (a) Original cantilever; (b) semicircular grooves were cut at both sides of the beam; (c) center parts and centers of the thinnest part were hollowed



Fig. 5 Photo of the cantilever with a spring constant of 1378 N/m

respectively. The corresponding vertical elastic deformation of the cantilever was detected by the laser displacement sensor. The deformation was plotted as a function of the standard loads in Fig. 6. The spring constant was

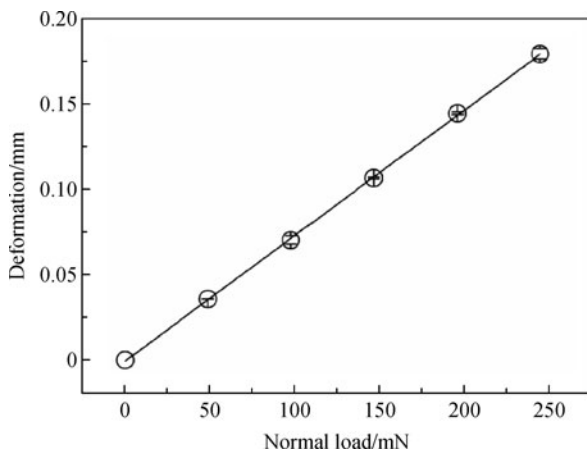


Fig. 6 Calibration of the spring constant

calibrated as 1378 N/m, which was very closed to the calculated value 1560 N/m.

After the calibration, the cantilever was fastened to the motorized goniometer stage (Zolix, model TSAG10-W, China). The goniometer can rotate in a range of $\pm 10^\circ$ with a precision of 0.00032° . The laser displacement sensor stands straightly on the base board through a magnetic holder, as shown in Fig. 2. The precise contact can be realized by operating the XYZ linear stage. When the computer indicates that the contact happens, the operator should keep moving the sample upward until the contact force meets the preset value.

3.3 Scanning actuation

The position of the sample can be adjusted preliminarily by two XY motors, whose minimum step length is $0.625 \mu\text{m}$ under eight segments. They can drive the sample to move a distance of 50 mm along the rail, which is large enough to cover a 1.8 inch silicon wafer. By programming the movement traces, various patterns can be fabricated on the samples. It should be noted that the route of the individual step is a short line. By entering the analytic function of a curve, the sliding traces can be resolved as an arrangement of short lines so that various curves can be obtained.

For example, the route of ellipse shown in Fig. 7 can be replaced by many interpolation lines. The analytic equation of the ellipse is

$$\frac{(x-sx-a)^2}{a^2} + \frac{(y-sy)^2}{b^2} = 1. \tag{1}$$

Here, the point (sx, sy) is the initial position, a is the semi-major axis of ellipse, b is the semi-minor axis of ellipse.

For the upper half ellipse, X coordinates of the starting points and the terminal points of interpolation lines are

$$x_{1i} = sx + (i-1)\Delta x, i = 1,2,3,\dots, \tag{2}$$

where Δx is the interpolation distance. Y coordinates of the starting points and the terminal points of interpolation lines can be determined by

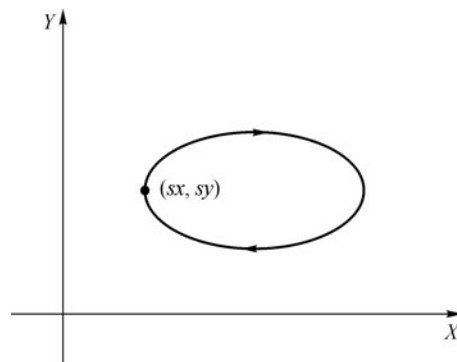


Fig. 7 Route of ellipse with a initial position at (sx, sy)

$$y_{1i} = sy + \frac{b}{a} \sqrt{a^2 - (x_{1i} - sx - a)^2}, \quad i = 1, 2, 3, \dots \quad (3)$$

Similarly, for the lower half ellipse, X coordinates of the starting points and the terminal points of interpolation lines are

$$x_{2j} = sx + (j-1)\Delta x, \quad j = 1, 2, 3, \dots \quad (4)$$

Y coordinates of the starting points and the terminal points of interpolation lines can be determined by

$$y_{2j} = sy - \frac{b}{a} \sqrt{a^2 - (x_{2j} - sx - a)^2}, \quad j = 1, 2, 3, \dots \quad (5)$$

Take the analytic results in X , Y arrays:

$$X = \{sx, x_{11}, x_{12}, \dots, x_{1i}, \dots, sx, x_{21}, x_{22}, \dots, x_{2j}, \dots\}, \quad (6)$$

$$Y = \{sy, y_{11}, y_{12}, \dots, y_{1i}, \dots, sy, y_{21}, y_{22}, \dots, y_{2j}, \dots\}. \quad (7)$$

Coordinates of the X , Y arrays stand for the starting points and the terminal points of every interpolation lines. If the values of a , b and Δx are designed, the sample can be driven by the motors along the trace of given ellipse.

Additionally, a manual XYZ linear stage (Zolix, model TSMW25R-XYZ-1AL, China) was fastened on the top of two motors. The “L-like” sample stage was fixed to the XYZ linear stage, by which the three dimensional position of sample can be controlled.

Based on above three key designs, friction-induced fabrication can be practiced by this apparatus. The capability of the apparatus was demonstrated by the following experiments.

4 Operation procedure and friction-induced fabrication on silicon

The friction-induced fabrication was carried out on Si(100) surface. Before the fabrication, the Si substrate was dipped in 20% HF solution for 3 min to remove native oxide layer. The complete fabrication flow is shown as below.

Firstly, place the HF-passivated Si sample on the “L-like” stage, and move the XYZ linear stage to locate the sample under the multi-probe array. Secondly, set the fabrication parameters in control system and program the movement traces according to the demanded patterns. Thirdly, approach the sample to the probe arrays and perform the friction-induced fabrication. After the friction-induced process, etch the sample by 20% wt.% KOH and isopropyl alcohol (IPA) (volume ratio = 5:1) aqueous solution [15,16]. Finally, the topography of the products can be observed by 3D map dual profile-meter (aep Technology, NanoMap-D, USA).

Based on the friction-induced fabrication method, the apparatus can be used for fabricating surface texture of silicon solar cells. As shown in Fig. 8, checked squares

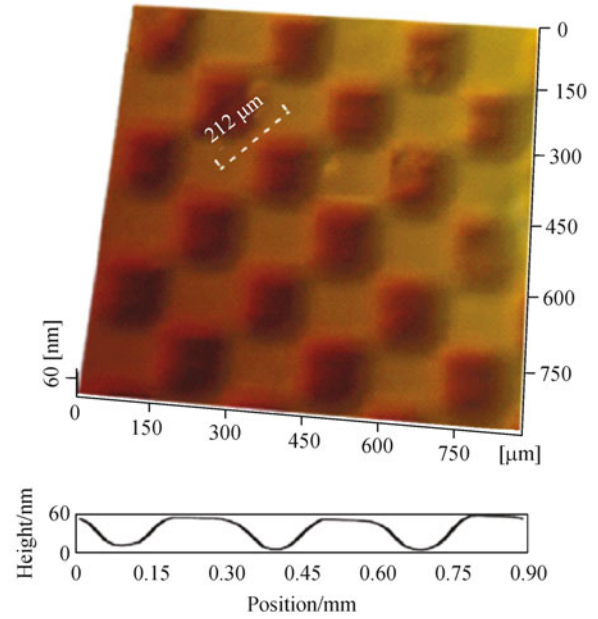


Fig. 8 Checked squares fabricated by scanning-scratch under $F_n = 1000$ mN with a 2×2 probe array and etching in the KOH and isopropyl alcohol (IPA) aqueous solution for 6 min

were fabricated by scanning-scratch under $F_n = 1000$ mN with a 2×2 probe array. The steel balls of $160 \mu\text{m}$ in radii were mounted together as a $212 \mu\text{m}$ square. The scan area was set as $150 \mu\text{m} \times 150 \mu\text{m}$, and the scan center was adjusted cycle by cycle with a $424 \mu\text{m}$ step length. The complete scanning-scratch consists of 150 repeated bidirectional line-scratches. After the scanning, the sample was etched in the KOH and isopropyl alcohol (IPA) aqueous solution for 6 min. The average height of the square was about 60 nm. Such surface textured silicon has a larger specific surface area and lower reflectivity, and it can possibly improve the energy exchange efficiency of solar cells [17].

As shown in Fig. 9, the grating can also be fabricated by this apparatus. By using the line-scratch mode, line array was fabricated under the applied normal load $F_n = 500$ mN with a 1×2 probe array. The distance between the adjoining tips was $80 \mu\text{m}$. After etching in KOH and isopropyl alcohol (IPA) aqueous solution for 6 min, the average height of the line array was about 50 nm. During the scanning, the contact pressure P_c was calculated to be 2.4 GPa. It was reported that the tribochemical oxidation and mechanical deformation can result in a mask layer on Si [18]. This experimental result suggested that a contact pressure of 2.4 GPa was enough to create the etching mask on silicon surface.

Curved line was also achieved by the ellipse model in Fig. 7. Both of the values of a and b were set as $170 \mu\text{m}$, so the fabricated ellipse structure was a ring. The value of interpolation distance Δx was $1 \mu\text{m}$, which was precise

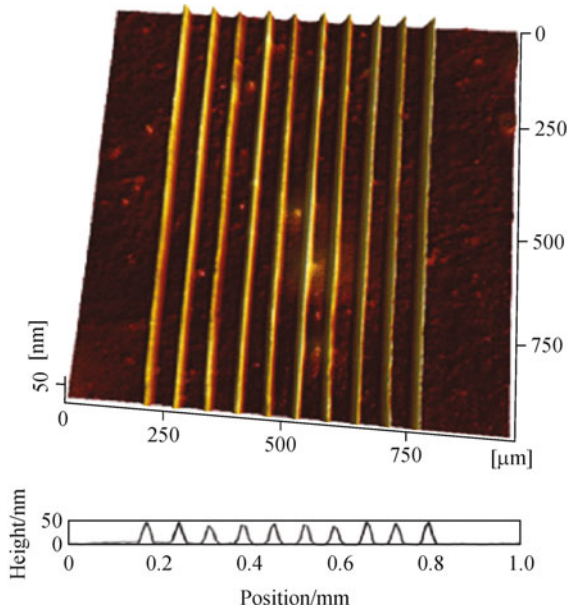


Fig. 9 Line array fabricated by scratching under $F_n = 500$ mN with a 1×2 probe array and etching in the KOH and isopropyl alcohol (IPA) aqueous solution for 6 min

enough to form a ring. As shown in Fig. 10, the radius of the ring was $170 \mu\text{m}$.

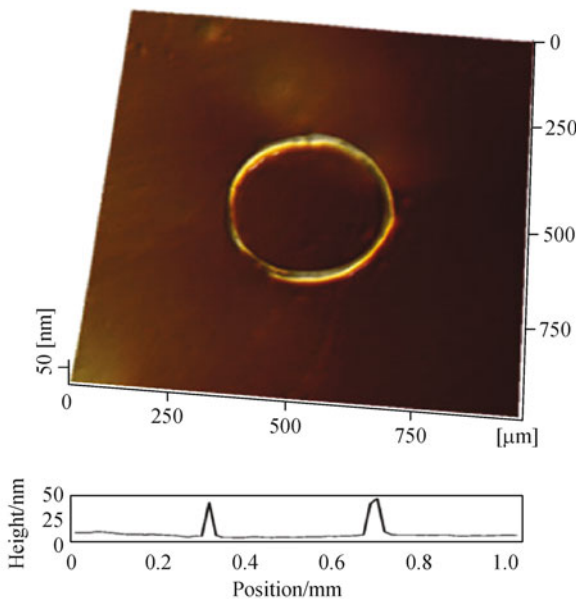


Fig. 10 Ring fabricated by scratching under $F_n = 250$ mN with a single probe and etching in the KOH and isopropyl alcohol (IPA) aqueous solution for 6 min

In summary, a multi-probe micro-fabrication apparatus was designed for friction-induced micro/nano fabrication on silicon. With a multi-points contact, the fabrication efficiency can be improved evidently than that of the

common single point contact. Compared with the traditional photolithography, the mask-independent fabrication flow in this paper is greatly simplified. Unlike the tip-induced local oxidation, the friction-induced method simply relies on sliding on the surface. In addition, this apparatus can be potentially used on the fabrication of the surfaces of insulative quartz and glass. The present results will not only enrich the friction-induced fabrication theory, but also encourage the surface texturing engineering.

5 Conclusions

A multi-probe micro-fabrication apparatus was designed based on the friction-induced fabrication method. The main parts of the equipment include actuating device, loading system, and control system. With the actuating device, the scanning can be realized over a $50 \text{ mm} \times 50 \text{ mm}$ area with a sliding speed of 10 mm/s . The fabrication loads was applied by a deformable parallelogram cantilever with a high precision. Multi-probe array was easily prepared by locating the steel micro balls into the indents array. The friction-induced process can be controlled and monitored by the software control system. Using this apparatus, line array, checked squares and curved structures were produced by friction-induced scanning and post etching in KOH. The fabrication flow based on multi-probe apparatus was greatly simplified and the fabrication efficiency was clearly improved. It will encourage the development of friction-induced fabrication method and shed new light on the texture engineering.

Acknowledgements The authors are grateful for the financial support from the National Basic Research Program (No. 2011CB707604) and the National Natural Science Foundation of China (Grant Nos. 90923017 and 51175441).

References

1. Bhushan B. Nanotribology and nanomechanics of MEMS/NEMS and BioMEMS/BioNEMS materials and devices. *Microelectronic Engineering*, 2007, 84(3): 387–412
2. Blumenthal M D, Kaestner B, Li L, Giblin S, Janssen T J B M, Pepper M, Anderson D, Jones G, Ritchie D A. Gigahertz quantized charge pumping. *Nature Physics*, 2007, 3(5): 343–347
3. Senn T, Bischoff J, Nüsse N, Schoengen M, Löchel B. Fabrication of photonic crystals for applications in the visible range by nanoimprint lithography. *Photonics and Nanostructures—Fundamentals and Applications*, 2011, 9(3): 248–254
4. Schiff H. Nanoimprint lithography: An old story in modern times? A review. *Journal of Vacuum Science & Technology B: Microelectronics and Nanometer Structures*, 2008, 26(2): 458–480
5. Srivastava S K, Kumar D, Vandana, Sharma M, Kumar R, Singh P K. Silver catalyzed nano-texturing of silicon surfaces for solar cell applications. *Solar Energy Materials and Solar Cells*, 2012, 100:

33–38

6. Sharma S N, Bhagavannarayana G, Sharma R K, Lakshmi Kumar S T. Role of surface texturization in the formation of highly luminescent stable and thick porous silicon films. *Materials Science and Engineering B*, 2006, 127(2–3): 255–260
7. Lan H B, Ding Y C, Liu H Z, Lu B H. Review of template fabrication for nanoimprint lithography. *Journal of mechanical engineering*, 2009, 45(6): 1–13
8. Silverman P J. Extreme ultraviolet lithography: overview and development status. *Journal of Microlithography, Microfabrication, and Microsystems*, 2005, 4(1): 011006
9. Yu B J, Dong H S, Qian L M, Chen Y F, Yu J X, Zhou Z R. Friction-induced nanofabrication on monocrystalline silicon. *Nanotechnology*, 2009, 20(46): 465303
10. Song C F, Li X Y, Yu B J, Dong H S, Qian L M, Zhou Z R. Friction-induced nanofabrication method to produce protrusive nanostructures on quartz. *Nanoscale Research Letters*, 2011, 6(1): 310
11. Park J W, Lee S S, So B S, Jung Y H, Kawasegi N, Morita N, Lee D W. Characteristics of mask layer on (100) silicon induced by tribonanolithography with diamond tip cantilevers based on AFM. *Journal of Materials Processing Technology*, 2007, 187–188: 321–325
12. Bhushan B. Nanoscale tribophysics and tribomechanics. *Wear*, 1999, 225–229: 465–492
13. Qian L M, Luengo G, Douillet D, Charlot M, Dollat X, Perez E. New two-dimensional friction force apparatus design for measuring shear forces at the nanometer scale. *Review of Scientific Instruments*, 2001, 72(11): 4171–4177
14. Wang J H, Jin G D, Cao S F. Research of strain in-measurement sensor based on double cantilever beam. *Chinese Journal of Sensors and Actuators*, 2005, 18(3): 589–595
15. Guo J, Song C F, Li X Y, Yu B J, Dong H S, Qian L M, Zhou Z R. Fabrication mechanism of friction-induced selective etching on Si(100) surface. *Nanoscale Research Letters*, 2012, 7(1): 152
16. Youn S W, Kang C G. Effect of nanoscratch conditions on both deformation behavior and wet-etching characteristics of silicon (100) surface. *Wear*, 2006, 261(3–4): 328–337
17. Zhong S H, Liu B G, Xia Y, Liu J H, Liu J, Shen Z N, Xu Z, Li C B. Influence of the texturing structure on the properties of black silicon solar cell. *Solar Energy Materials and Solar Cells*, 2013, 108: 200–204
18. Zhang L C, Zarudi I. Towards a deeper understanding of plastic deformation in mono-crystalline silicon. *International Journal of Mechanical Sciences*, 2001, 43(9): 1985–1996